International Journal of Energy Policy and Management
2018; 3(1): 29-40
http://www.aascit.org/journal/ijepm
ISSN: 2472-9477 (Print); ISSN: 2472-9493 (Online)

AASCIT American Association for Science and Technology

Parametric Cost Analysis and Optimization of a Cryogenic Adsorption System for Helium-Hydrogen Separation

Dibyendu Bandyopadhyay, Rupsha Bhattacharyya*, Sandeep Kannuparambil Chandrasejgaran

Heavy Water Division, Bhabha Atomic Research Centre, Mumbai, India

Email address

rupshabhattacharyya1986@gmail.com (R. Bhattacharyya), rupsha@barc.gov.in (R. Bhattacharyya)

*Corresponding author

Citation

Dibyendu Bandyopadhyay, Rupsha Bhattacharyya, Sandeep Kannuparambil Chandrasejgaran. Parametric Cost Analysis and Optimization of a Cryogenic Adsorption System for Helium-Hydrogen Separation. *International Journal of Energy Policy and Management.* Vol. 3, No. 1, 2018, pp. 29-40.

Received: January 1, 2018; **Accepted:** February 3, 2018; **Published:** March 14, 2018

Abstract: Separation of hydrogen and its isotopes from helium gas is a necessary operation in the context of fusion energy systems. One of the techniques available for this separation is selective cryogenic adsorption of hydrogen on microporous adsorbents like molecular sieves (MS). In this work, adsorption isotherm data at 77 K for hydrogen on four kinds of commercially available molecular sieves have been experimentally obtained and fitted to the Langmuir isotherm. The adsorption isotherms and the constant pattern breakthrough model has been used to determine the breakthrough time and length of the mass transfer zone, and hence the size of an adsorbent bed for a given breakthrough hydrogen concentration. The cost of hydrogen adsorbed has been obtained by considering the cost of adsorbent, adsorption vessel, nitrogen boil-off losses and gas pumping costs. The effect of variation of parameters like adsorbent particle type, size, gas velocity through the bed, feed hydrogen concentration on the normalized cost of the adsorption system per adsorption cycle per mole of hydrogen adsorbed was studied. These parametric studies allowed determination of preliminary design parameters of the most economical adsorption system for hydrogen-helium separation, based on the entire adsorption process and using minimal experimental data.

Keywords: Cryogenic Adsorption, Molecular Sieves, Cost Analysis, Hydrogen Helium Separation, Parametric Optimization

1. Introduction

The separation of hydrogen and its isotopes from helium gas is an important step in the proposed fusion energy systems such as the ITER project in Cadarache, France [1]. Helium is the commonly used coolant and purge gas for recovery of hydrogen isotopes from solid and liquid breeder blankets placed along the walls of the plasma chamber of fusion reactors. Hydrogen isotopes must be recovered by separation from helium gas before they can be fed back as fuel to the plasma chamber for subsequent plasma pulses. Thus the helium is also purified before it is recycled back to the breeder blankets. The composition of the hydrogen-helium stream can be highly variable depending upon the source or origin, ranging from less than 1% hydrogen in helium (e.g. helium used as purge gas in the breeder blankets) to greater than 90% (e.g. in the permeate from palladium based membrane or membrane reactor units).

One of the widely applied methods for hydrogen isotope separation from helium is cryogenic adsorption technology [2]. Highly porous adsorbents like carbon or zeolite based molecular sieves (MS) can selectively adsorb and immobilize industrially significant amounts of hydrogen gas and its isotopes selectively at very low temperature of about 77 K, while allowing the unadsorbed helium gas to pass through the adsorber bed. The adsorbed beds can be regenerated and the pure hydrogen can be recovered by allowing them to be warmed up to room temperature or beyond (e.g. 150-250 deg C) in a thermal swing adsorption (TSA) scheme. Alternatively the bed pressure can be lowered using a

vacuum pump which will allow the hydrogen isotopes to be evacuated and collected externally in a pressure swing adsorption scheme (PSA) [3]. A combination of these two techniques can also be used to optimally exploit their intrinsic advantages.

A number of studies have been performed to obtain cryogenic hydrogen adsorption isotherm and kinetic data, both of which are required for the design of an adsorption column for hydrogen-helium separation [4]. Cryogenic adsorption has been proposed as the method for helium purification as well, by removing trace amounts of impurities like oxygen, nitrogen and even hydrogen [1].

In this work, a design and optimization methodology for obtaining the least cost cryogenic adsorption system for hydrogen recovery from helium for a given throughput and feed concentration has been described. The method can be applied for rapidly obtaining preliminary, cost optimized design parameters with minimal prior experimental studies. Cryogenic adsorption isotherms of hydrogen have been obtained experimentally to determine the adsorption capacities of different zeolite based molecular sieves (viz. MS 3A, MS 4A, MS 5A and MS 13X) at 77 K as function of hydrogen pressure. The adsorption bed has been designed on the basis of the numerically obtained breakthrough curves by assuming 'constant pattern behaviour' [5]. Adsorption kinetics (convective mass transfer in the gas phase as well as gas diffusion inside the porous adsorbents) has therefore been incorporated in the design of the adsorber bed, instead of just using the saturation capacity data of particular adsorbents. Parametric optimization has been carried out to obtain design and operating parameters such that the normalized total cost per unit quantity of hydrogen adsorbed (i.e. the sum of fixed and operating costs) per cycle of the cryogenic adsorption system is the minimum, based on the adsorption cycle only. All cost data used for the calculations are for the year 2017. The influence of different feed concentrations on the selection of optimal parameters has also been studied. The sensitivity of the cost to various parameters has also been examined.

2. Adsorption Isotherms

A commercially available volumetric sorption type instrument was used to determine the cryogenic adsorption isotherms for pure hydrogen on four commercially available zeolites, in the form of cylindrical pellets of uniform size. An average value of 2.5 was taken as the measure of the tortuosity in the porous adsorbents based on reported literature, in the absence of specific data from our experiments or from literature [6, 7].

The working principle of this instrument is based on volumetric sorption method in batch mode and the findings can be used for determining adsorption isotherm at a constant temperature (77 K in the present study). At NVT condition, the equilibrium pressure of the system depends on the adsorption capacity of the adsorber material for a particular adsorbent gas and this idea has been implemented in this instrument. Before carrying out the experiment, the available volume of the system (burette, inner volume and piping) was measured by using blank analysis. Molecular sieve of a particular type (weight of each sample was about 1-1.5 gm) was filled into glass sample burette. The burette loaded with MS was then heated at 473 K for 10 hours under vacuum to remove residual water, different organic moieties and any traces of adsorbed gases of previous experiment. Then the filled sample burette was immersed deep into liquid nitrogen container (77 K). The burette was isolated from vacuum system by closing the isolation valve. Burette valve was opened to introduce small fixed quantity hydrogen gas at each pulse and from then system pressure was being observed. In between two pulses sufficient time was allowed to reach adsorption equilibrium which was further confirmed by checking the pressure of the system and the equilibrium pressure of each pulse was recorded in the storage system. The entire procedure was carried out automatically, based on user inputs provided during each run. From the injected volume and corresponding equilibrium pressure, adsorbed volume as a function of pressure was calculated. This isotherm was used to calculate the total adsorption capacity of the adsorber material, normalized by the weight of sample placed in the burette for each run. For evaluating the BET surface area of these molecular sieves, the standard experimental technique by using nitrogen adsorption on the molecular sieves at -197°C was carried out.

The experimentally obtained isotherm data were fitted to an equation having the form of the Langmuir isotherm (Eqn 1) and the two best fit parameters for each adsorbent were obtained at 77 K through least squares regression analysis. The adsorption isotherms are presented in Figure 1 and the empirical constants are shown in Table 1. It is observed that MS 4A has the highest hydrogen uptake capacity at a given hydrogen pressure, out of the four adsorbents considered in this work, particularly at the higher hydrogen pressure end of the spectrum.

$$\frac{q}{q^*} = \frac{KC}{1+KC} \tag{1}$$

Table 1. *Langmuir isotherm parameters and adsorbent data for cryogenic hydrogen adsorption (77 K) on various adsorbents.*

Adsorbent	q* (g mol/g)	K (litre/g mol)	R^2	r_p (A°)	a_s (m^2/g)	τ
MS 3A	$5.496*10^{-3}$	45.25	0.949	1.5	343	2.5
MS 4A	$6.062*10^{-3}$	59.22	0.926	2.0	347	
MS 5A	$5.892*10^{-3}$	67.01	0.935	2.5	572	
MS 13X	$5.907*10^{-3}$	56.27	0.958	5.0	569	

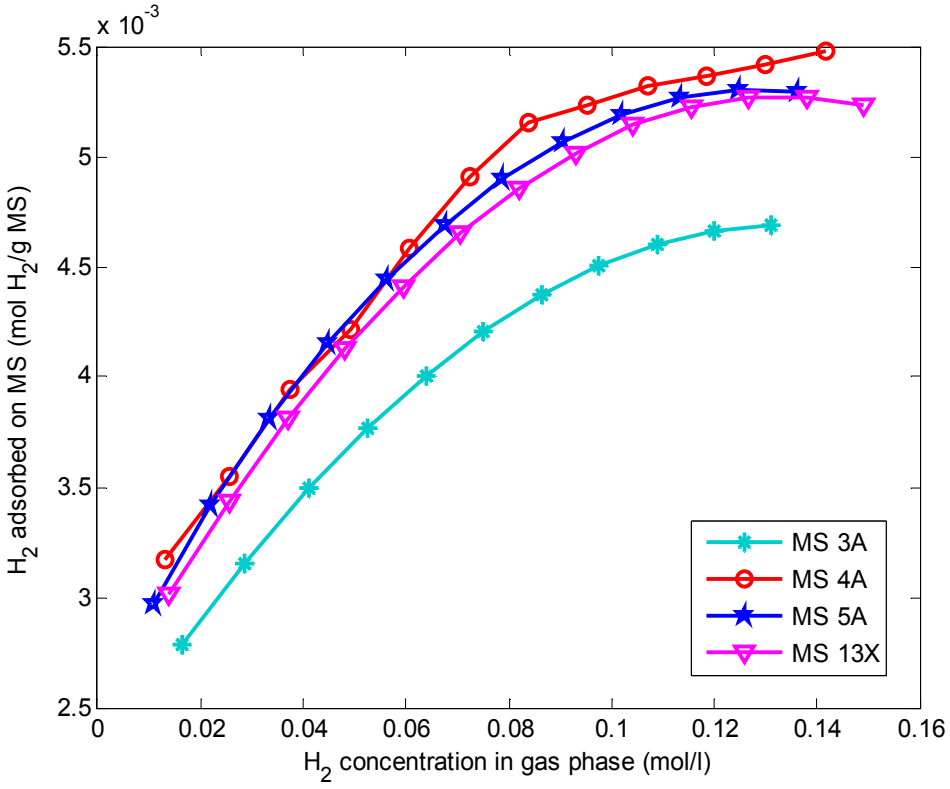

Figure 1. *Hydrogen adsorption isotherms on different molecular sieves at 77 K.*

3. Model Equations for Adsorption System Sizing and Cost Calculations

The adsorbent bed was designed using the local equilibrium model [9] and by theoretically evaluating the constant pattern concentration front generated during the adsorption step. This led to estimation of the breakthrough curve through the bed, breakthrough time, bed saturation time as well as the approximate velocity of the wave front. The experimentally determined parameters of the adsorption isotherms were used in this calculation and adsorption kinetics was modeled using well known convective mass transfer and pore diffusion correlations for external and internal mass transport respectively. Axial dispersion and the effect of pressure drop on adsorber performance were neglected. It was later established that pressure drop is negligible for the conditions considered in this work. The adsorber bed was assumed to operate isothermally and the heat of adsorption released was assumed to be lost entirely to the liquid nitrogen used to maintain the cryogenic conditions, which leads to nitrogen boil-off losses.

The length of the equilibrium section of the bed was determined from the feed conditions and adsorption isotherm and calculated breakthrough time, assuming the solid adsorbent bed to be in equilibrium with hydrogen in the feed gas at the gas-solid interface. The length of the mass transfer zone was evaluated next from the breakthrough curve. The actual bed length was taken as the sum of the lengths of the equilibrium section and the mass transfer zone, to provide a margin of safety in design and to take care of uncertainties in the evaluated quantities and model assumptions [10]. Gas properties were evaluated as volumetric average of hydrogen and helium properties, based on the arithmetic mean of inlet and outlet gas mixtures at breakthrough. The concentration front was numerically evaluated from Eqn. (2) as follows, along with Eqns. (3)-(5), for an adsorption system described by the Langmuir isotherm [9]:

$$\frac{1+KC_o}{KC_o}\boldsymbol{ln}\frac{C}{C_1}+\frac{1}{KC_o}\boldsymbol{ln}\frac{C_o-C_1}{C_o-C}=\frac{k_m\bar{a}C_o}{(1-\varepsilon_b)\rho_p q_o}(t-t_1) \quad (2)$$

$$k_m\bar{a}=\left[\frac{1}{k_c\bar{a}}+\frac{r_o^2}{60D_e m'(1-\varepsilon_p)\rho_p}\right]^{-1} \quad (3)$$

$$\frac{k_c d_p}{D_{AB}}=2+1.1(Sc)^{\frac{1}{3}}(Re_p)^{0.6} \quad (4)$$

$$D_e=\frac{\varepsilon_p}{\tau}\left[\frac{1}{\left(\frac{1}{D_{AB}}\right)+\left(\frac{1}{D_k}\right)}\right] \quad (5)$$

The diffusivity of hydrogen through helium gas was estimated from the Chapman-Enskog equation [9].

The velocity of the concentration wave front was obtained by [9]

$$u_{SH}=\frac{u}{1+\frac{1-\varepsilon_b}{\varepsilon_b}\rho_p\frac{\Delta q}{\Delta C}} \quad (6)$$

Pressure drop through the adsorption bed was calculated using the Ergun equation [11]:

$$\frac{\Delta P}{l}=\frac{150\mu(1-\varepsilon_b)^2u}{\varepsilon_b^3 d_p^2}+\frac{1.75(1-\varepsilon_b)\rho u^2}{\varepsilon_b^3 d_p} \quad (7)$$

Due to progressive adsorption of hydrogen in the adsorbent bed, the total gas flow rate through the bed varies significantly with time and position in the bed, especially when the feed stream is rich in hydrogen. Thus conservatively, the pressure drop is calculated using the maximum superficial velocity based on gas flow rate at the inlet. This gives us an estimate of the maximum pumping costs for the gas through the adsorption bed.

Bed voidage for a given particle size was calculated from [12]

$$\boldsymbol{\varepsilon_b = 0.4 + 0.05\left(\frac{d_p}{D}\right) + 0.412\left(\frac{d_p}{D}\right)^2 for\ \frac{d_p}{D} < 0.5} \quad (8)$$

Knudsen diffusivity was calculated using the following equation [13]:

$$\boldsymbol{D_K = 0.97 * r_p\sqrt{\left(\frac{T}{M}\right)}} \quad (9)$$

Surface diffusion has been neglected in calculating effective diffusivity in the hydrogen-molecular sieve system. The relative importance of external and internal mass transfer resistances in the overall adsorption kinetics can be established by calculating the Biot number as $\frac{k_c d_p}{2D_e}$ for each set of parameters.

The value of ā was evaluated as [9]

$$\boldsymbol{\bar{a} = \frac{6(1-\varepsilon_b)}{d_p}} \quad (10)$$

The hydrogen gas pressures in adsorption data were converted to equivalent concentration units at 77 K using the following relation:

$$\boldsymbol{C = \frac{p}{RT}} \quad (11)$$

The total quantity (i.e. moles) of hydrogen adsorbed on the adsorbent material at the end of the bed saturation or equilibration time for a given adsorption cycle can be calculated as [10]

$$W_{H2} = Q * C_o \int_0^{t_e}(1 - \frac{C}{C_o})dt \quad (12)$$

Thus, W_{H2} for each case can be evaluated from the calculated breakthrough curve.

The total number of cycles (N_c) for the adsorbent bed has been calculated on the basis of initial ITER start up, commissioning and operation in H-H fusion mode with this trial phase continuing for at least two years [20, 21]. It is expected that the hydrogen isotope recovery systems (of which the cryogenic hydrogen adsorption bed is a component) will be available at that time for testing even though there will not be direct requirement for the system. Based on the bed saturation time in each case and an assumed 6 hours for bed warm-up and thermal regeneration, the total number of cycles has been determined and the total gas pumping cost and nitrogen boil-off losses for all these cycles taken together have been evaluated and included in the cost function to be minimized. Based on this each bed is expected to undergo about 3000-4000 cycles of adsorption and desorption in the course of 2 years.

The design and operating parameters for the adsorbent bed considered in this work are as shown in Table 2. Adsorbent particles were assumed to be uniform spheres and their cost was assumed to be the same for all particle sizes of a given adsorbent. Bed diameter was calculated for each assumed superficial velocity for the given throughput and the length of the bed was taken as the sum of the length of the mass transfer zone and length of saturated bed in each case. Thus the total bed volume and the amount of adsorbent required were obtained.

Table 2. *Base case design, operating and cost parameters for hydrogen-helium separation column.*

Parameter	Value/Range
Bed temperature	77 K
Inlet Pressure	1.5 bar (a)
Vessel design pressure	15 bar (a)
Hydrogen volume per cent in feed mixture	10%-90%
Breakthrough hydrogen concentration at bed exit	0.1% of feed concentration
Concentration of hydrogen at bed exit when bed is assumed saturated	99.9% of feed concentration
Volumetric flow rate of gas mixture	1 $Nm^3\ hr^{-1}$
Gas superficial velocity	0.1-1.0 m s^{-1}
Adsorbent particle equivalent diameter	1-5 mm
Adsorbent particle density	1100 kg m^{-3}
Cost of electricity per unit	₹ 10/kWhr
Cost of adsorbent material	MS 3A: ₹ 7842/kg [14] MS 4A: ₹ 3177/kg [14] MS 5A: ₹ 9582/kg [14] MS 13X: ₹ 9662/kg [14]
Cost stainless steel	₹ 500/kg [15]
Density of material of construction of the reactor (SS 316L)	7800 kg m^{-3} [15]
Motor efficiency	0.85
Pump efficiency	0.60
Heat of vapourization of liquid nitrogen at 77 K	5.95 kJ/mol N_2 [16]
Average heat of adsorption of hydrogen on molecular sieve adsorbents	9.89 kJ/mol H_2 [17] = 4.945 kJ/gm H_2 adsorbed
Cost of liquid nitrogen	₹ 40/L [18]
Vessel design pressure	20 bar
Maximum allowable stress of stainless steel at 77 K	10 MPa [19]

Costs of the vessel, adsorbent material, gas pumping through the bed per adsorption cycle and replacement of liquid nitrogen lost by boil-off were subsequently obtained. Typical values of pump and motor efficiencies were considered for analysis, without reference to details of particular types of pumps for this application. Nitrogen boil-off rate was calculated by assuming the entire heat of adsorption released during the adsorption cycle is taken up by the liquid nitrogen surrounding the adsorber bed. The total cost per adsorption cycle per unit amount of hydrogen adsorbed for a given feed composition (which is the objective function for cost minimization) is thus expressed as follows:

$$C_t = \frac{(W_b C_c + W_a C_a + \frac{\Delta P l Q t_e N_c}{(36*10^5*3600\eta_m\eta_p)} + N_c[C_{N2} Q C_o \Delta H_{ads} \int_o^{te}(1-\frac{C}{C_o})dt]/\lambda_{N2})}{N_c Q C_o \int_0^{te}(1-\frac{C}{C_o})dt} \quad (13)$$

The weight of the vessel (and hence its cost) was calculated after evaluation of the vessel wall thickness as follows [22]:

$$thk = \frac{P_d D}{2\sigma J - P_d} \quad (14)$$

$$W_b = \pi D * thk * l * \rho_s \quad (15)$$

The independent decision variables used in evaluating the above objective function must have values within the ranges specified in Table 2. These ranges were selected based on practical engineering considerations and heuristics.

4. Parametric Cost Analysis and Optimization

4.1. Parametric Analysis and Optimization

The design and operating parameters of the cryogenic adsorption system that can be independently selected include the adsorber tube diameter and hence gas superficial velocity, adsorbent type and adsorbent particle size. For the base case conditions of 50% hydrogen in the feed mixture, 3 mm adsorbent particles and gas superficial velocity of 0.99 m s^{-1}, the typical lengths of the adsorption column for different adsorbents are shown below in Table 3. The effects of varying these parameters on the overall cost of the adsorption system per mole of hydrogen stored per cycle have been shown in Figures 3-6. It is seen that the longest calculated breakthrough time is obtained with MS 3A, followed by MS 4A, MS 5A and MS 13X. While MS 4A has the highest adsorption capacity for hydrogen at a given partial pressure as seen from the adsorption isotherms in Figure 1, the breakthrough characteristics are primarily determined by adsorption kinetics (both external and internal mass transfer characteristics), particularly when the adsorption capacities are comparable as in the case of MS 4A and 5A. In this case, the slightly greater average pore size in MS 5A results in lower resistance to internal diffusion of hydrogen, a higher effective mass transfer coefficient and hence a shorter mass transfer zone and breakthrough time. From the calculated values of Biot number for the adsorbents over the entire parameter space, it was found that the values ranged from $1*10^3$ to $2*10^4$, which indicates that internal mass transfer resistances govern the overall adsorption kinetics (and therefore the design of the adsorption column) and external mass transfer characteristics have negligible effect on the process.

Table 3. *Length of mass transfer zone in base case cryogenic adsorption of hydrogen on molecular sieves.*

Adsorbent	Velocity of mass transfer zone (m/s)	Time for bed saturation (s)	Length of mass transfer zone (m)	Length of equilibrium section (m)
MS 3A	0.0298	213.98	6.37	11.45
MS 4A	0.0256	151.06	3.87	6.95
MS 5A	0.0258	118.34	3.05	5.48
MS 13X	0.0265	63.37	1.68	3.02

Figure 3 shows that for a given adsorbent and identical breakthrough hydrogen concentration for all adsorbents, the cost of the adsorption system decreases with increasing hydrogen concentration in the feed gas as the higher concentration of hydrogen offers a greater driving force for mass transfer, leading to lower bed lengths and overall costs. For a given feed hydrogen concentration, MS 3A leads to the most expensive system, followed by MS 13X and MS 5A. System cost for MS 4A are found to be significantly lower than those for the other adsorbents.

Figure 4 shows that for any given adsorbent, the cost rises with increasing particle diameter. This is because larger diameter adsorbents offer greater resistance to mass transfer, creating low effective mass transfer coefficients and hence increased mass transfer zone widths and overall bed lengths. Gas pumping cost being a negligible part of the total cycle cost due to very low pressure drops in the scenarios considered here, higher particle size therefore offers no cost advantage to the adsorption system in terms of savings in pumping power and act only to slow down adsorption rates and increase system size and cost.

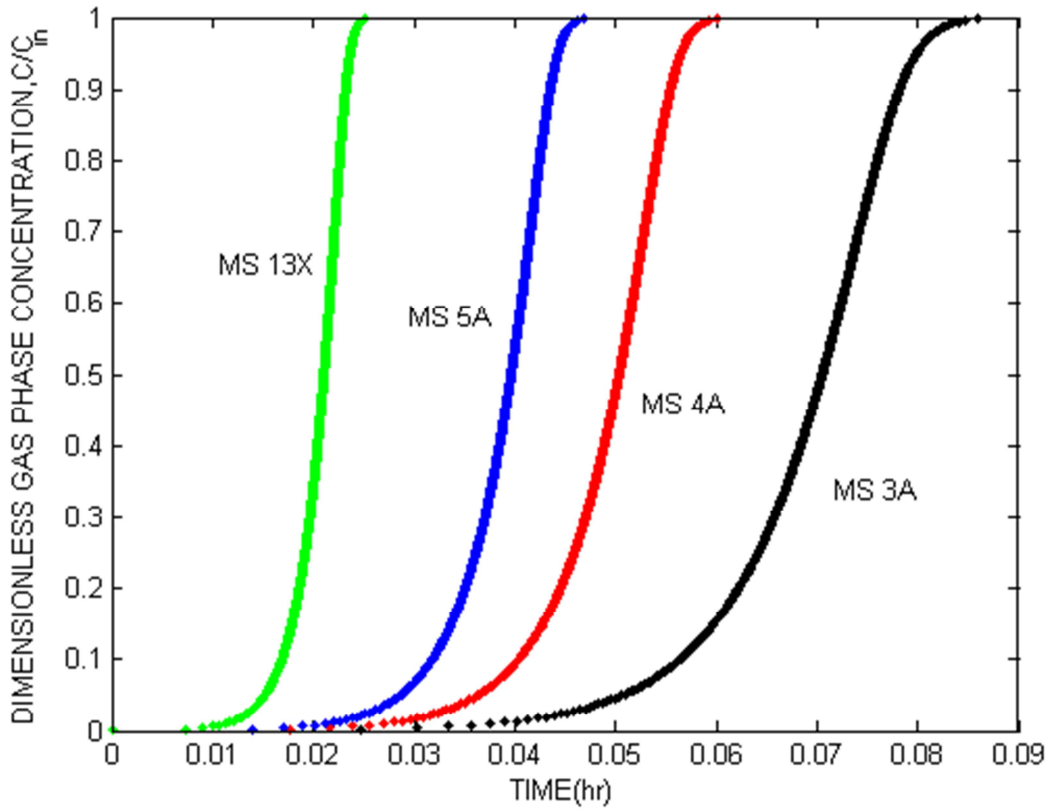

Figure 2. *Representative breakthrough curves for hydrogen adsorption on different molecular sieves at 77 K (d_p = 3 mm, 50% hydrogen in the feed mixture, u = 0.99 m/s).*

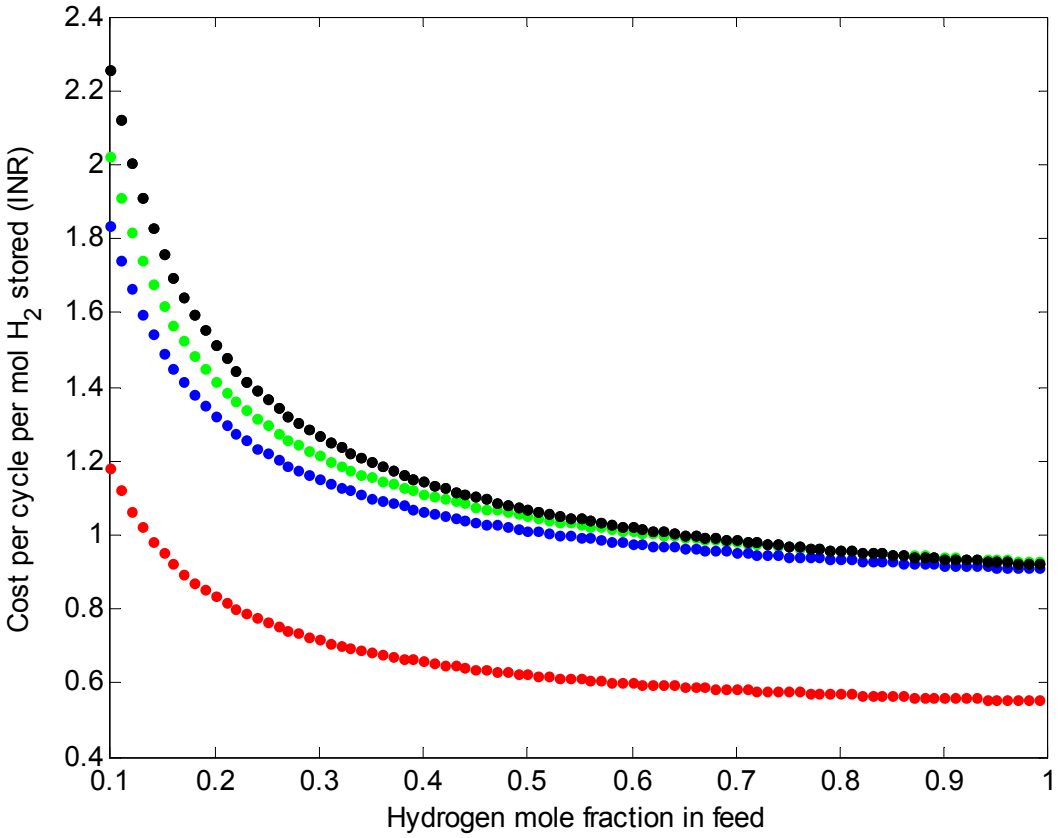

Figure 3. *Effect of hydrogen concentration in feed gas on the cryogenic adsorber system cost (● MS 3A ● MS 4A ● MS 5A ● MS 13X, d_p = 0.003 m, u = 0.99 m/s).*

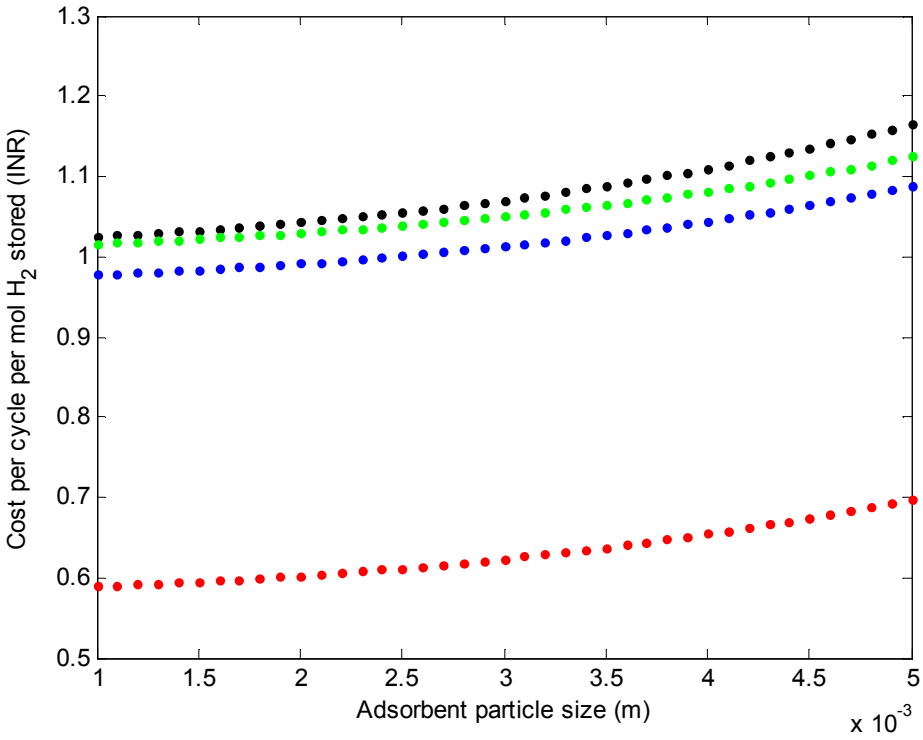

Figure 4. *Effect of adsorbent particle size on the cryogenic adsorber system cost (● MS 3A ● MS 4A ● MS 5A ● MS 13X, y_{H2} = 0.5, u = 0.99 m/s).*

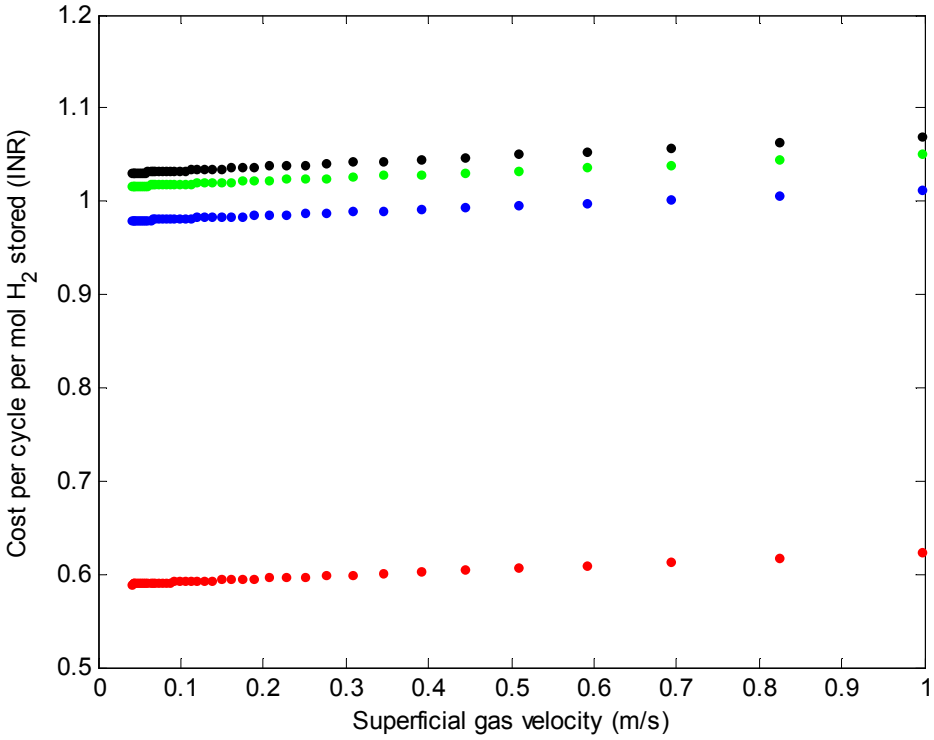

Figure 5. *Effect of gas velocity on the cryogenic adsorber system cost (● MS 3A ● MS 4A ● MS 5A ● MS 13X, y_{H2} = 0.5, d_p = 0.003 m).*

As seen in Figure 5, increasing bed diameter for given adsorbent particle size decreases gas superficial velocity and bed voidage, and overall there is a decrease of gas interstitial velocity, when the gas throughput is kept constant. Thus the effective mass transfer coefficient decreases when the bed diameter decreases and the time taken for the mass transfer zone to cross its own length increases. But the concentration wave front velocity also decreases significantly and hence the length of the mass transfer zone decreases. The length of the equilibrium section of the bed also decreases and this leads to an overall reduction in the size and cost of the adsorber system. But as the overall adsorption kinetics are primarily

dependent on internal mass transfer resistances, the variation of cost with changes in the external mass transfer conditions is quite small, as seen from the nearly flat profiles in Figure 5 and Figure 6 presents the adsorption system cost as a function of bed diameter instead of the corresponding superficial gas velocity as in Figure 5.

For each adsorbent material considered, systematic parametric analysis was carried out to identify the conditions which lead to least overall adsorber system cost per mol H_2 adsorbed per adsorption cycle. A set of typical results are presented in Table 4. It is observed that in the feed hydrogen concentration range of 10 to 90% by volume, the optimal bed diameter is 0.05 m and particle size is 1 mm for each adsorbent considered here. For a given hydrogen per cent in feed, adsorber systems based on MS 4A leads to the lowest costs, over the entire range of concentrations. The cost of gas pumping and nitrogen lost due to boil off are negligibly small for the throughputs considered here. These figures increase if gas volumetric flow rate is enhanced keeping the same diameter of the adsorber vessel but the variation in the normalized adsorber system cost is quite small and may be neglected, even when there is a two orders of magnitude increase in the feed throughput over that considered in the base case conditions.

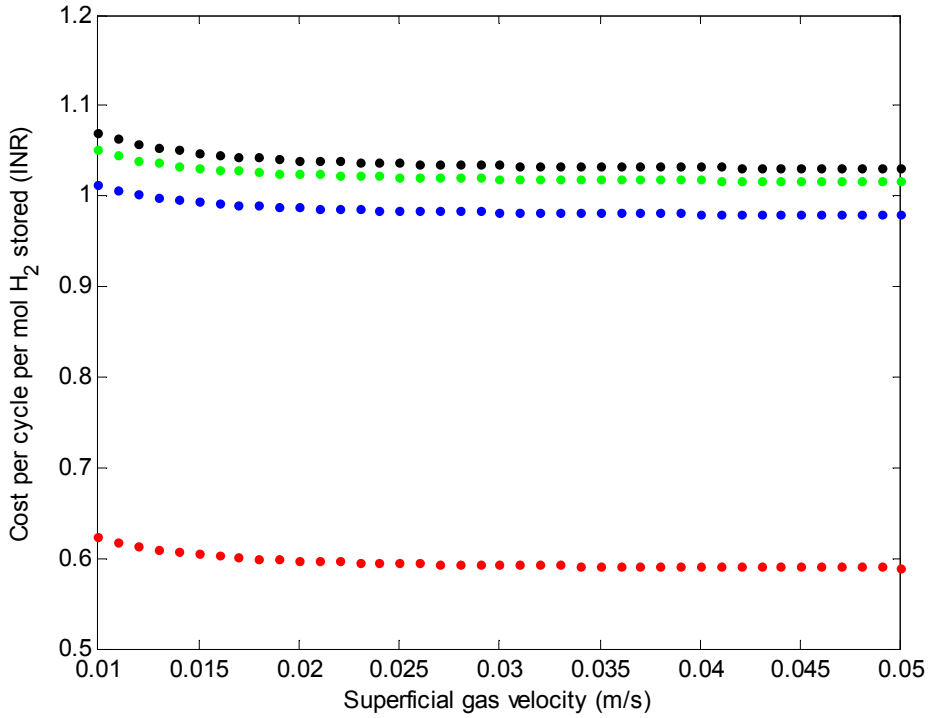

Figure 6. *Effect of bed diameter on the cryogenic adsorber system cost (● MS 3A ● MS 4A ● MS 5A ● MS 13X, y_{H2} = 0.5, d_p = 0.003 m).*

Table 4. *Optimal parameters for cryogenic hydrogen adsorber system.*

Adsorbent	Feed hydrogen concentration (%)	Optimal bed diameter (m)	Optimal particle size (mm)	Adsorber system cost (INR/mol H_2 adsorbed/cycle)
	10	0.05	1	2.121
	25	0.05	1	1.295
MS 3A	50	0.05	1	1.019
	75	0.05	1	0.923
	90	0.05	1	0.894
	10	0.05	1	1.098
	25	0.05	1	0.713
MS 4A	50	0.05	1	0.584
	75	0.05	1	0.540
	90	0.05	1	0.525
	10	0.05	1	1.752
	25	0.05	1	1.168
MS 5A	50	0.05	1	0.972
	75	0.05	1	0.906
	90	0.05	1	0.884
	10	0.05	1	1.939
	25	0.05	1	1.245
MS 13X	50	0.05	1	1.012
	75	0.05	1	0.933
	90	0.05	1	0.906

4.2. Sensitivity Analysis

The results presented in the previous sections demonstrate the effect of some of the most important factors on the adsorber system cost for hydrogen-helium separation. A more detailed consideration of the other individual factors that can potentially affect the system cost and their relative importance has been presented in this section. The representative adsorption system considered here is based on MS 4A. A sensitivity analysis taking into account the independent variables mentioned in Table 2, with an assumed variation of ± 20% in the values of each from the base case values has been carried out. This analysis enables one to identify opportunities for cost reduction as well identification of the major cost components. The results, indicating the deviation from the baseline cost in year 2017 are shown in Figure 7. The red segments represent the cost when the parameter under consideration is decreased by 20% and the blue segment represents the cost when that parameter is increased by 20%.

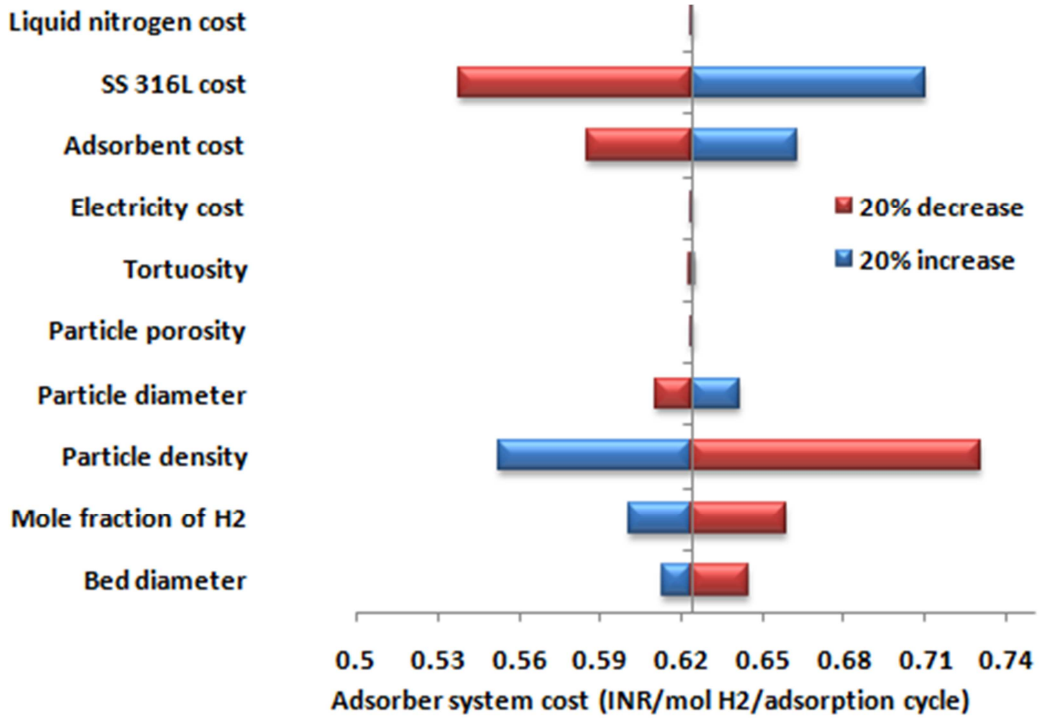

Figure 7. *Sensitivity of MS 4A based cryogenic hydrogen adsorption system cost to various parameters.*

It is observed that the total cost of the adsorber system is mostly influenced by the adsorbent bulk density, adsorbent cost, cost of the adsorber vessel's material of construction, the feed concentration of hydrogen and the adsorbent bed diameter and particle diameter. The microporous properties of a given adsorbent particle like particle porosity and tortuosity are seen to have negligible influence on the cost estimates, thus these need not be known with a very high degree of accuracy for the design and costing analysis. Liquid nitrogen cost also shows no influence on adsorption system cost in this study, thereby indicating that boil up losses of nitrogen under the conditions considered here do not seriously affect the cost patterns. The particle morphological parameters like internal porosity and tortuosity also have no direct effects on the system cost, even though they govern the internal mass transfer characteristics in the adsorbent material. It is the internal pore size which controls these characteristics and for a given kind of molecular sieve adsorbent, the internal porous network is highly regular and uniform and there is hardly any variation in pore size.

The contribution of the various cost elements to the total adsorption system cost per cycle (for base case design values) is shown in Figure 8. It is clear that for the base case feed flow rate, the fixed cost of the adsorbent material and adsorber vessel are the major two contributions, while the operating cost components in the form of liquid nitrogen cost and gas pumping cost have negligible influence on overall costs. When the feed flow rate through the base case column is increased 10 times to 10 $Nm^3\ hr^{-1}$, the overall normalized system cost becomes INR 1.2485 per cycle per mole of H_2 stored from INR 0.6239 per cycle per mole of H_2 (an increase by a factor of 2) and the relative contributions of the cost components also changes appreciably, as shown in Figure 9. This is because the total length of the column as well as the superficial velocity through it increases and pressure drop also rises accordingly. Thus gas pumping cost (which is proportional to the square of the superficial velocity and hence rises 100 times for a ten-fold rise in throughput through the same column) becomes much more significant in this case than the base case conditions. It also becomes necessary to account for the changing gas flow rate due to adsorption of hydrogen for higher flow rates in order to accurately represent the cost implications of higher throughput in a given adsorption column.

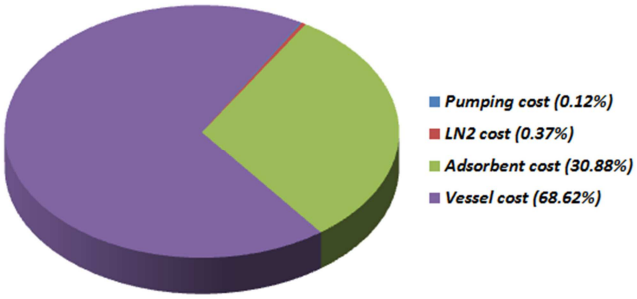

Figure 8. *Distribution of costs among various components of the MS 4A based cryogenic hydrogen adsorption system for 1 Nm^3 hr^{-1} feed flow rate.*

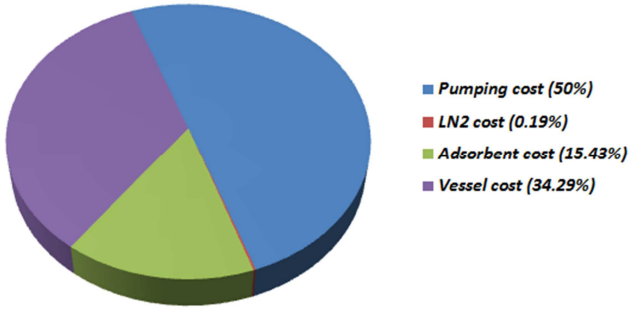

Figure 9. *Distribution of costs among various components of the MS 4A based cryogenic hydrogen adsorption system for 10 Nm^3 hr^{-1} feed flow rate.*

5. Results and Conclusion

This work presents a simplified approach to designing a cryogenic adsorption column for hydrogen-helium separation, using molecular sieve adsorbents which selectively take up hydrogen gas but not helium. Such columns may also be considered for helium purification by trace impurity removal. The design methodology is based on the constant pattern breakthrough curve concept and it requires minimal prior experimental work. Adsorption isotherms for hydrogen on MS 3A, 4A, 5A and 13X at 77 K and a maximum feed gas pressure of around 1 atm were obtained experimentally in this work. Using the adsorption isotherms and well known correlations for internal and external mass transfer, the breakthrough curves for cryogenic hydrogen adsorption in a fixed bed adsorber were determined. The lengths of the equilibrium section of the adsorber bed and the length of the mass transfer zone were then determined from the computed breakthrough curve. Parametric cost analysis was done considering the design parameters of the adsorber system, gas circulation requirements and liquid nitrogen boil off losses due to release of heat of adsorption.

The parametric analysis enabled us to identify the type of adsorbent and the adsorber system design parameters like adsorbent particle size and adsorber diameter that lead to the overall least cost cryogenic adsorption based hydrogen-helium separation system, on a per cycle and per unit quantity of hydrogen adsorbed basis. It is seen that no matter what the adsorbent material is, the least cost system is obtained by using particles of 1 mm diameter and bed diameter of about 0.05 m (~ 2”), according to applicable range of values of these variables as considered in this study. Bed diameters were so chosen to keep the gas velocity through the packed adsorption column between 0.1 to 1 m/s. MS 4A is the adsorbents which leads to the least cost systems, out of the 4 adsorbents considered here, for the entire range of hydrogen feed concentration. This is mainly due to the much lower cost of this adsorbent material compared with any of the others. Pressure drop and hence gas pumping requirements as well as nitrogen boil off losses were determined to have a negligibly small effect on the normalized cost of the system for the gas throughputs considered here. Parametric sensitivity analysis revealed that for any adsorbent, the cost is most sensitive to adsorbent density, cost of the vessel, price of adsorbent and feed hydrogen concentration. Morphological details of the adsorbent like internal porosity and tortuosity did not have much influence on system cost even though they govern internal mass transfer behaviour. Electricity costs and hence gas pumping costs were also quite insignificant compared to the other cost components for the base case, through the relative contributions of these components to the overall system cost changes with changes in throughput for a given column.

The methodology demonstrated here can be easily applied to arrive at the preliminary cost optimized design of any fluid-solid adsorption system provided adsorption isotherm data are available and mass transfer behaviour can be predicted with reasonable confidence using appropriate correlations.

Acknowledgements

The authors are thankful to Shri D Y Gaikwad, Heavy Water Division, BARC for his assistance throughout the course of the experimental work reported here and to Shri Kalyan Bhanja and Dr Sadhana Mohan, BARC for support and encouragement.

Funding

This research did not receive any specific grant from funding agencies in the public, commercial, or not-for-profit sectors.

Nomenclature

$\bar{a}$	Specific surface area of adsorbent solid, m^2 m^{-3}
a_s	Specific surface area of adsorbent solid, m^2 g^{-1}
C	Concentration of hydrogen in the gas stream at any time, mol l^{-1}
C_1	Breakthrough concentration of hydrogen at the exit, mol l^{-1}

C_a	Unit cost of adsorbent material, INR kg^{-1}
C_c	Unit cost of empty vessel, INR kg^{-1}
C_{N2}	Unit cost of liquid nitrogen, INR l^{-1}
C_o	Feed concentration of hydrogen in the gas stream, mol l^{-1}
C_t	Total cost of adsorption system, INR
D	Bed inside diameter, m
D_{AB}	Diffusivity of hydrogen through helium, m^2 s^{-1}
D_e	Effective diffusivity of gas in porous solid, m^2 s^{-1}
D_k	Knudsen diffusivity, m^2 s^{-1}
d_p	Adsorbent particle diameter, m
$\triangle H_{ads}$	Heat of adsorption of hydrogen on microporous material, kJ mol^{-1}
J	Joint efficiency, dimensionless
k_c	Convective mass transfer coefficient, m s^{-1}
k_m	Effective mass transfer coefficient considering pore diffusion, m s^{-1}
K	Constant in Langmuir adsorption isotherm,
l	Length of adsorption bed, m
m’	Average slope of the adsorption isotherm, l gm^{-1}
M	Molecular weight of diffusing gas inside pores, gm mol^{-1}
N_c	Total number of adsorption cycles carried out in the adsorbent bed, dimensionless
p	Partial pressure of hydrogen in the vessel at any time, Pa
P_d	Design pressure of adsorber bed, Pa
$\triangle P$	Pressure drop across the adsorbent bed, Pa
q	Quantity of hydrogen adsorbed on the solid, mol g^{-1}
q^*	Constant in Langmuir adsorption isotherm,
q_o	Quantity of hydrogen on the solid in equilibrium with feed gas, mol g^{-1}
Q	Gas volumetric flow rate through adsorber, m^3 s^{-1}
r_o	Particle radius, m
r_p	Pore radius, m
R	Universal gas constant, J mol^{-1} K^{-1}
Re_p	Particle Reynolds number, dimensionless
Sc	Schmidt number, dimensionless
t	Time, s
t_l	Breakthrough time during the adsorption cycle, s
t_e	Bed saturation/equilibration time for the adsorber bed, s
thk	Vessel wall thickness, m
T	Bed temperature, K
u	Gas interstitial velocity in the adsorber, m s^{-1}
u_{SH}	Mass transfer front propagation velocity, m s^{-1}
W_a	Total weight of adsorbent in the vessel, kg
W_b	Weight of adsorber vessel, kg
W_{H2}	Quantity of hydrogen adsorbed per cycle in the cryogenic adsorber bed, mol
ε_b	Bed voidage, dimensionless
ε_p	Particle voidage, dimensionless
λ_{N2}	Latent heat of vapourization of liquid nitrogen at 77 K, kJ mol^{-1}
η_m	Motor efficiency, dimensionless
η_p	Pump efficiency, dimensionless
μ	Viscosity of gas, Pa s
ρ_p	Solid density, kg m^{-3}
ρ	Gas density, kg m^{-3}
ρ_s	Steel density, kg m^{-3}
σ	Maximum allowable tensile strength of SS 316L at 77 K, Pa
τ	Tortuosity, dimensionless

References

[1] Fujimura K, Raffray AR, Abdou MA. Analysis of helium purge flow in a solid breeder blanket. Fus Eng Des 1989; 8: 109-114.

[2] Das NK, Kumar P, Mallick C, Bhandari RK. Development of a helium purification system using pressure swing adsorption. Curr Sci 2012; 103 (6): 632-634.

[3] Ruthven DM, Principles of adsorption and adsorption processes. 1st ed. New York: John Wiley and Sons; 1984.

[4] Qian X, Luo D, Huang G, Song X, Liu W. Experimental investigation on cryogenic hydrogen adsorption of molecular sieves. Int J Hydrogen Energy 2012; 87 (4): 359-362.

[5] Seader JD, Henley EJ, Roper DK, Separation Process Principles-Chemical and Biochemical Operations. 3rd ed. New Jersey: John Wiley & Sons; 2011.

[6] Kong W, Zhang Q, Xu X, Chen D. A Simple Expression for the Tortuosity of Gas Transport Paths in Solid Oxide Fuel Cells' Porous Electrodes. Energies 2015; 8: 13953-13957.

[7] Pisani L. Simple Expression for the Tortuosity of Porous Media. Trans Porous Med 2011; 88: 193-203.

[8] Molecular Sieves - Technical Information Bulletin, available at http://www.sigmaaldrich.com/chemistry/chemical-synthesis/learning-center/technical-bulletins/al-1430/molecular-sieves.html, last accessed on 05.10.2017.

[9] Dutta BK, Principles of Mass Transfer and Separation Processes. 1st ed. New Delhi: Prentice Hall of India Pvt. Ltd.; 2007.

[10] Geankoplis CJ, Transport Processes and Unit Operations. 3rd ed. New Jersey: Prentice Hall International, Inc.; 1993.

[11] McCabe W, Smith J, Harriott P, Unit Operations of Chemical Engneering. 7th ed. Boston: McGraw Hill Companies, Inc.; 2005.

[12] Yang WC, Flow through Fixed Beds, in W. C. Yang, (Ed.); Handbook of Fluidization and Fluid-Particle Systems. 1st ed., New York: Marcel Dekker Inc.; 2003.

[13] Froment GF, Bischoff KB, Chemical Reactor Analysis and Design. 1st ed. New York: John Wiley and Sons; 1979.

[14] Molecular Sieves, available at http://www.sigmaaldrich.com/programs/research-essentials-products.html?TablePage=14577469, last accessed on 05.10.2017.

[15] Latest Price 316 304 316L Stainless Steel Pipe 2016-2017, available at http://www.ashtapadoverseas.com/blog/stainlesssteelpipe-sspipe/, last accessed on 17.10.2017.

[16] About Liquid Nitrogen, available at https://technifab.com/cryogenic-resource-library/cryogenic-fluids/liquid-nitrogen/, last accessed on 17.10.2017.

[17] Schmitz B, Müller Ulrich, Trukhan N, Schubert M, Ferey G, Hirscher M. Heat of Adsorption for Hydrogen in Microporous High-Surface-Area Materials. Chem Phys Chem 2008; 9: 2181-2184.

[18] Price of Liquid Nitrogen, available at https://hypertextbook.com/facts/2007/KarenFan.shtml, last accessed on 17.10.2017.

[19] Botshekan M, Degallaix S, Desplanques Y, Polak J. Tensile and LCF properties of AISI 316LN SS at 300 and 77 K. Fatigue Fract Engg Matl Struct 1998; 21: 651-660.

[20] What is ITER?, available at https://www.iter.org/proj/inafewlines#6, last accessed on 13.11.2017.

[21] Polevoi AR, Campbell DJ, Chuyanov VA, Houlberg W, Ivanov AA, Kukushkin AS, Lamalle P, Loarte A, Mukhovatov VS, Oikawa T. Assessment of plasma parameters for the low activation phase of ITER operation. Nucl. Fusion 2013; 53: 123026-123032.

[22] Moss D, Pressure Vessel Design Manual. 3rd ed. Oxford: Gulf Professional Publishing; 2004.